Synthesis and Characterization of Copper Oxide Nanoparticles

A Thesis submitted

In Partial Fulfilment of the Requirements
for the degree of

MASTER OF SCIENCE

in

PHYSICS

BY

Praveen Jha

(Roll No: 30704011)

SCHOOL OF PHYSICS AND MATERIALS SCIENCE
THAPAR UNIVERSITY
PATIALA-147004
INDIA
July 2009

CERTIFICATE

This is to certify that the thesis entitled "**Synthesis and Characterization of Copper Oxide Nanoparticles"** submitted by Mr. Praveen Jha is in partial fulfillment for degree of Master of Science in Physics in this University. This work has been done under my supervision. He has not submitted this material for credit towards any other degree at this or any other university.

July 15, 2009

(**Dr. S. D. Tiwari**)
Lecturer
School of Physics and Materials Science
Thapar University, Patiala,

Countersigned by

Dr. O. P. Pandey
Prof & Head
School of Physics and Materials Science
Thapar University, Patiala

Dr. R. K. Sharma
Dean of Academic Affairs
Thapar University, Patiala

DECLARATION

I hereby declare that the thesis entitled **"Synthesis and Characterization of Copper oxide nanoparticle"** is the original work carried out by me under the supervision of Dr. S. D.Tiwari. The matter embodied in this thesis has not been submitted anywhere else for the award of any degree

Praveen Jha

ACKNOWLEDGEMENT

All of first I would like to thank my thesis supervisor Dr. S. D. Tiwari for his valuable guidance during the course of this work. I really appreciate him for his help, patience, discussions with me and encouragements.

I acknowledge Dr. K. P. Rajeev for providing X-ray diffraction, thermogravimetric analysis, differential thermal analysis and magnetization measurements data used in this thesis. I thank Mr. Vijay Kumar Bisht for his help at different stages of the work.

I acknowledge Dr. Amjad Ali for allowing me to use his lab facilities. I am also thankful to Dinesh and Amit Vashishth for their help during the sample preparation. I thank my room partner Baljeet for his help during the course of this thesis.

I am also thankful to my all classmates for their help and support at every stage during the thesis work.

I owe my sincere gratitude to my parents and brother whose support and obstinate love gave me the energy to complete this thesis work successfully and also for their untiring help during the difficult moment.

Praveen Jha

ABSTRACT

$Cu(OH)_2$ is prepared by a sol-gel method and characterized by X-ray diffraction, differential thermal analysis, thermogravimetric analysis and vibrating sample magnetometer. The $Cu(OH)_2$ is found to decompose into CuO on heating. Nanocrystalline and bulk CuO samples are prepared by heating the $Cu(OH)_2$ at 300 and 1000 ^{0}C respectively. The $Cu(OH)_2$, nanocrystalline CuO and bulk CuO are found to be antiferromagnetic at room temperature. The magnetization of CuO is found to increase with decreasing crystallite size.

CONTENTS

LIST OF FIGURES

CHAPTER-1
INTRODUCTION

The work on magnetism in nanoscale particles has become a very interesting area of research because of their properties and technological applications [1]. In nanoparticles of antiferromagnetic materials the surface spins dominate in the magnetization measurements due to their lower coordination [2]. The fraction of surface spins increases with decreasing particle size. Because of this reason the magnetization per unit mass of antiferromagnetic particles increases with decreasing particle size. Variations in the magnetic properties of such particles are expected due to change in the relative number of surface spins.

1.1 Magnetism - A Brief Idea

All matters are composed of atoms and atoms are composed of protons, neutrons and electrons. The protons and neutrons are located in the atomic nucleus and the electrons are in constant motion around the nucleus. Electrons carry a negative charge and produce a magnetic field as they move through space

Each electron has magnetic moments that originate from two sources. The first is the orbital motion of the electron around the nucleus and the second is its spin. In an atom the orbital magnetic moments of some electron pairs cancel each other. The same happens with the spin magnetic moments. The overall magnetic moment of the atom is thus the sum of all of the magnetic moments of the individual electrons. For the case of a completely filled electron shell or subshell, the magnetic moments completely cancel out each other. Thus only atoms with partially filled electron shells have a magnetic moment [3, 4]. The magnetic properties of materials are determined by the nature and magnitude of the atomic magnetic moments. Several forms of magnetic behaviors have been observed in different materials. These are diamagnetism, paramagnetism, ferromagnetism, antiferromagnetism and ferrimagnetism.

Diamagnetism is a very weak form of magnetism and observed only in the presence of an external magnetic field. It is the result of changes in the orbital motion of electrons due to the external magnetic field. The induced magnetic moment is very small and in a direction opposite to that of the applied field. When placed between the poles of a

strong electromagnet, diamagnetic materials are attracted towards regions where the magnetic field is weak. Diamagnetism is found in all materials, however because it is so weak it can only be observed in materials that do not exhibit other forms of magnetism. Superconductors, example of perfect diamagnets, are expelled by an external magnetic field.

Paramagnetism is observed in those materials which contain non interacting magnetic moments. In presence of external magnetic field these moments try to align along the field direction. Susceptibility of paramagnetic materials is described by the Curie law. Paramagnetic behavior can also be observed in other magnetic materials that are above their Curie or Néel temperature.

Ferromagnetic materials are strongly attracted by a magnetic filed. In these materials the magnetic moments interact with each other and are aligned in same direction. This alignment of the magnetic moments in ferromagnetic materials results in a strong permanent internal magnetic field inside the material. It is this strong internal magnetic field that causes the ferromagnetic materials to be attracted by a magnetic field. While the interaction between the moments tends to align adjacent moments but usually all of the moments do not point in the same direction throughout the material. In reality the material consists of a number of regions called domains. Within each domain the magnetic moments are aligned in same direction and the various domains may or may not be aligned in same direction. Above a transition temperature, known as the Curie temperature, a ferromagnetic material becomes paramagnetic.

In antiferromagnetic materials the magnetic moments align themselves in a antiparallel arrangements throughout the material so that it does not exhibit any significant magnetism in absence of external magnetic field. Above a critical temperature, known as the Neel temperature, the antiferromagnetic material becomes paramagnetic.

In a ferrimagnetic material the magnetic moment of the atoms on different sub lattices are opposite in direction, as in antiferromagnetism. But the magnitudes of the

magnetic moments on different sub lattices are not equal and a spontaneous magnetization remains. Above a transition temperature, known as Curie temperature, the ferrimagnetic materials become paramagnetic.

1.2 Nanoparticles of Magnetic Materials

Nanoparticles of any materials can be prepared by reducing all its three dimensions to nanometer range. Nanoparticles of magnetic materials are of great interest for researchers from a wide range of disciplines [1], including magnetic fluids, catalysis, biotechnology, magnetic resonance imaging and data storage. Synthesized magnetic nanoparticles give rise to a variety of different physical and chemical properties largely depending on the synthesis method and chemical structure.

Sufficiently small particles of magnetic materials behave like a giant paramagnetic moments with a fast response to applied magnetic fields with negligible remanence and coercivity. This is known as superparamagnetism [5, 6]. In other words the superparamagnetism is a phenomenon by which magnetic materials may exhibit a behavior similar to paramagnetism at temperatures below the Curie or the Néel temperature.

The magnetic anisotropy energy per particle, which is responsible for pointing the particle magnetic moments along a certain direction, is expressed as

$$E(\theta) = KV \sin^2 \theta,$$

where K is anisotropy constant, V is volume of the particle and θ is the angle between the magnetization direction and the easy axis. The energy barrier $K\,V$ separates the two energetically identical easy axes. For sufficiently small particle the thermal energy $k_B\,T$ exceeds the energy barrier $K\,V$ and the direction of magnetization is easily changed. If the thermal energy is larger than the anisotropy energy (i.e. $K\,V$) then the system behaves like a paramagnetic material. However in this case there are giant moments of particle instead of atomic magnetic moments.

1.3 Antiferromagnetic Copper Oxide

The transition metal monoxides MnO, FeO, CoO, NiO, and CuO are antiferromagnetic in nature. MnO, FeO, CoO, and NiO have NaCl structure. But the CuO has a monoclinic unit cell [7]. The antiferromagnetic ordering in CuO is due to the exchange interaction between Cu^{+2} ions via O^{-2} ions. The lattice parameters for CuO are a = 4.6837Å, b = 3.4226 Å, c = 5.1288 Å, α = 90°, β = 99.54° and γ = 90° [8]. In the crystal the copper ions is coordinated by 4 oxygen ions in an approximately square planar configuration.

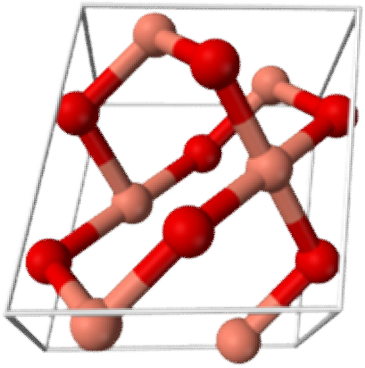

Fig. 1.1: Unit cell of CuO. Copper ions (shown by light brown) are coordinated by 4 oxygen ions (shown by dark red) in an approximately square planar configuration [8].

1.4 Organization of Thesis

- Chapter - 1 is introductory in nature. It introduces the basic concepts of magnetism and its origin.
- Chapter - 2 deals with experimental part of the thesis. In this chapter the synthesis of copper hydroxide and various characterization techniques used are discussed.
- Chapter - 3 discusses the results of the various experiments performed.
- Chpater - 4 concludes the thesis and also gives the scope for future work.

CHAPTER-2
EXPERIMENTAL DETAILS

In this chapter detailed procedure for the synthesis of $Cu(OH)_2$ and all the used experimental techniques are discussed.

2.1 Sol-Gel Method of Synthesis

There are various techniques [9] to prepare nanocrystals like sputtering, laser ablation, cluster deposition, sol-gel method etc. In the present work the synthesis of $Cu(OH)_2$ is preferred by a sol-gel route because this method is easy and economical.

The sol-gel process [10] involves the formation of a colloidal suspension (sol) and gelation of the sol to form a network in a continuous liquid phase (gel). The precursors for synthesizing these colloids consist usually of a metal or metalloid element surrounded by various reactive ligands. The starting material is processed to form a sol in contact with water or dilute acid. Removal of the liquid from the sol yields the gel, and the sol to gel transition controls the particle size and shape.

Nanocrystalline and bulk CuO are prepared by thermal decomposition of freshly prepared $Cu(OH)_2$ at different temperatures. The $Cu(OH)_2$ is prepared by reacting aqueous solutions of 0.1 *M* copper nitrate, $Cu(NO_3)_2.3\ H_2O$ and 0.5 *M* sodium hydroxide. For this NaOH solution is added drop wise with constant stirring until the pH of the system reaches to 12. The chemical reaction between copper nitrate and sodium hydroxide solutions is as follows.

$$Cu(NO_3)_2 + 2\ NaOH \rightarrow Cu(OH)_2 + 2\ NaNO_3$$

The resulting blue-green gel is washed several times with distilled water until free of nitrate ions. Finally the gel is dried by heating at 100 ^{0}C for 10 hours. Copper hydroxide decomposes into copper oxide on heating as follows.

$$Cu(OH)_2 \rightarrow CuO + H_2O$$

In this work bulk and nanocrystalline CuO samples are prepared by heating the copper hydroxide in air for 3 hours at different temperatures.

2.2 Characterization Techniques

X-ray diffractometer, differential thermal analyzer, thermogravimetric analyzer and vibrating sample magnetometer are used to characterize the prepared samples.

2.2.1 X-ray Diffraction

A crystal is made up of family of lattice planes consisting of periodic array of lattice points [3]. The set of parallel planes are designated by Miller indices. When an X-ray strikes a family of planes, it will be reflected as shown in Figure 2.1.

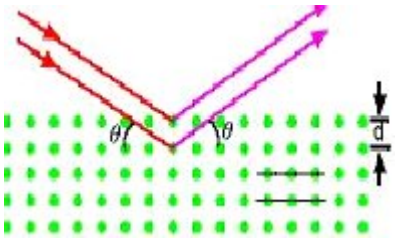

Fig. 2.1: X-ray beam reflected by the set of parallel planes.

The reflected rays from different planes interfere with each other and the resultant intensity distribution is modified. For crystalline materials the diffracted waves consist of sharp interference maxima. The positions of peaks in an X-ray diffraction pattern are directly related to the atomic distances. The wavelength λ of the X-ray, the spacing d between lattice planes and angle of reflection θ are related as

$$2\, d \sin\theta = n\, \lambda$$

where n = 1, 2, …. This is known as Bragg's law. Using this relation the d values of the material can be calculated.

2.2.2 DTA and TGA

In differential thermal analysis (DTA) the sample and an inert reference material are heated under identical conditions. The temperature difference between the sample and

reference material is continuously recorded during this process. The difference in temperatures is then plotted against temperature. By this the changes in the sample due to the absorption or evolution of heat can be detected.

Systematic sketch of a DTA is shown in Figure 2.2 [11]. It mainly consists of sample holder, thermocouples, furnace, temperature programmer and recording system. The sample holder is in form of a crucible and usually made of platinum. The thermocouples are not placed in direct contact with the sample to avoid contamination and degradation. The furnace should provide a stable hot zone. The temperature programmer is required to obtain desire constant heating rates.

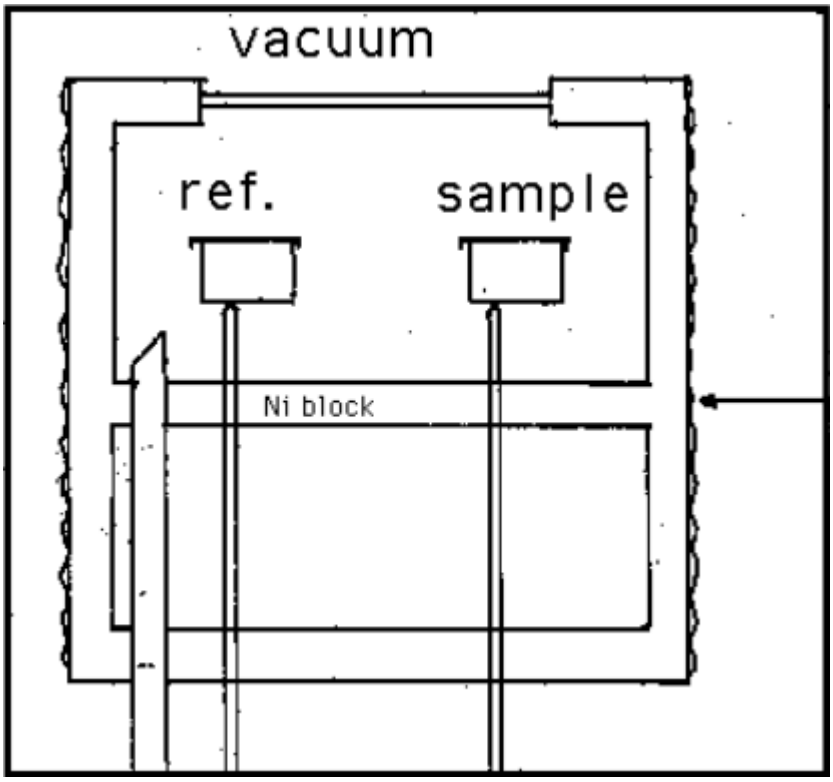

Fig. 2.2: Schematic diagram of a DTA cell [11].

The main applications of DTA are in finding transition temperature, heat capacity, identification of materials etc. An endothermic or exothermic transition will give rise to a

peak in the DTA curve. The endothermes are along negative direction and exotherms are along positive direction in the plot.

Thermogravimetric analysis (TGA) is an analytical technique used to determine the thermal stability and fraction of volatile components in a material by monitoring the weight change that occurs as the material is heated. The measurement is normally carried out in air or in an inert atmosphere and the weight is recorded as a function of increasing temperature. The maximum temperature is selected so that the specimen weight is stable at the end of the experiment.

2.2.3 Vibrating Sample Magnetometer

Vibrating sample magnetometer (VSM) is an instrument that measures magnetization of a sample [12]. For this a sample is placed inside a uniform magnetic field to magnetize it. This magnetized sample is allowed to vibrate vertically inside a pickup coil. This will cause an electric field across the pickup coil according to Faraday's Law of Induction. The induced voltage/current across the pickup coil is proportional to the magnetization of the sample. The various components are hooked up to a computer interface. Using controlling and monitoring software, the system can tell us that how much the sample is magnetized.

CHAPTER-3
RESULTS AND DISCUSSION

3.1 Thermal Analysis

Many compounds are not stable at higher temperatures and decompose into other compounds on heating. Keeping this thing in mind the prepared green colored powdered sample is characterized with the help of a thermogravimetric and differential thermal analyzer.

3.1.1 Thermogravimetric Analysis

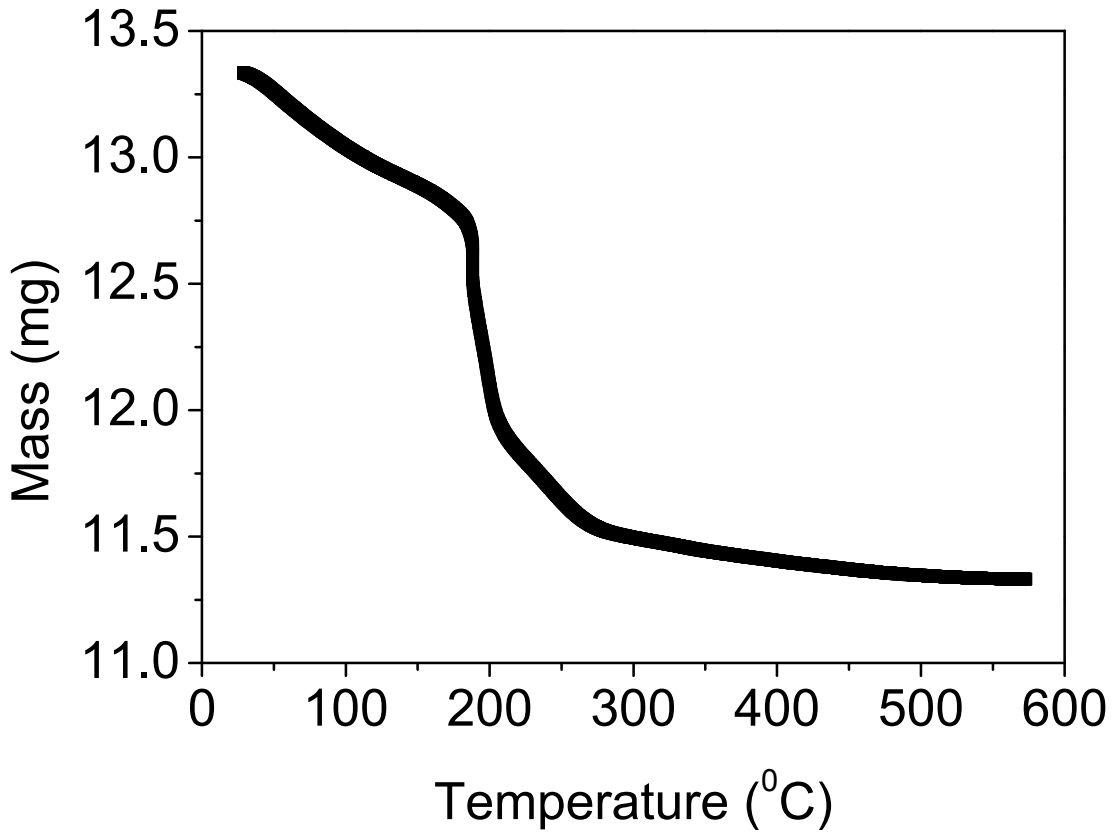

Fig. 3.1: Variation of mass of the prepared sample as a function of temperature.

In thermogravimetric analysis the mass of a given material is measured as a function of temperature by keeping the material at a constant heating rate. The prepared green colored powder sample is heated at a rate of 10 ^{0}C per minute for this analysis. The

variation of mass of the sample as a function of temperature is shown in Figure 3.1. This figure shows that the mass of the sample decreases with increasing temperature continuously with a sudden change in mass at around 200 ^{0}C. After further heating the mass of the material becomes almost constant. This analysis tells about the possibility of a change in phase of the sample.

3.1.2 Differential Thermal Analysis

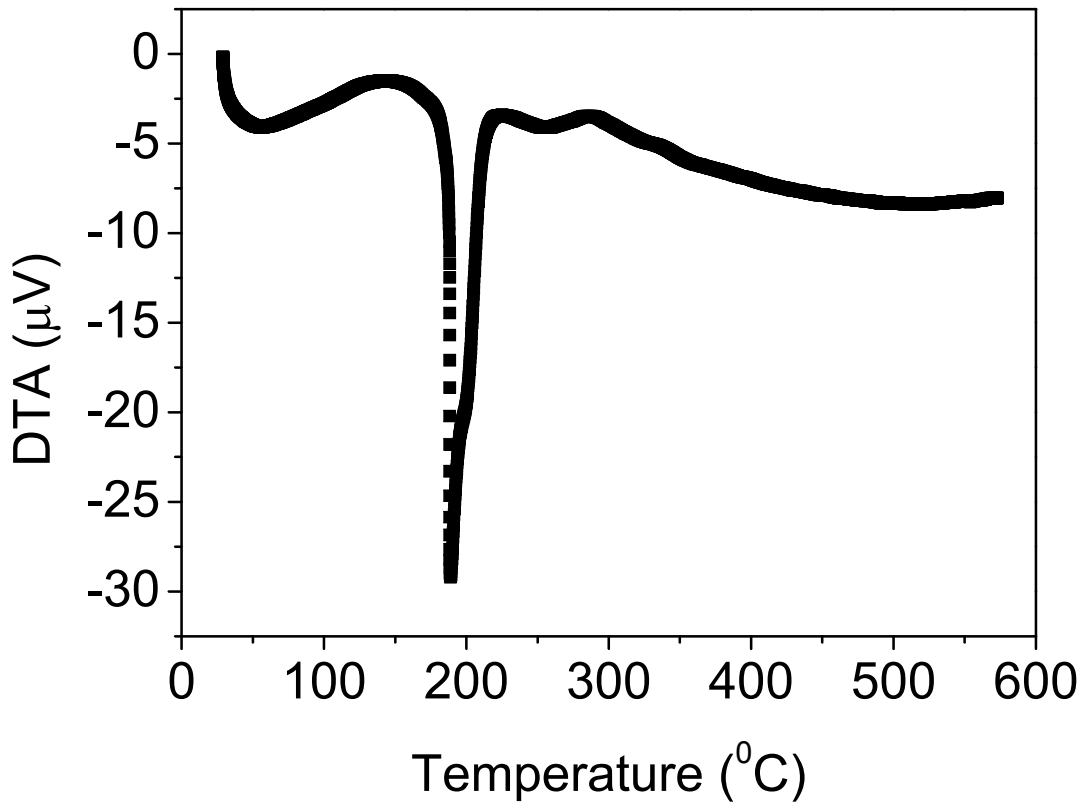

Fig. 3.2: Differential thermal analysis curve for the prepared sample.

In differential thermal analysis the temperature difference between a given material and a reference material is measured as a function of temperature by keeping the given material and the reference material at a constant heating rate. This variation, recorded

at a constant heating rate of 10 ^{0}C per minute, is shown in Figure 3.2. This figure shows that there is very intense endothermic peak at about 200 ^{0}C. The intense endothermic peak in this analysis again indicates about the possibility of phase change in the material at about 200 ^{0}C.

Thus the thermogravimetric analysis and the differential thermal analysis indicate for a possibility of a change in the phase of the material at about 200 ^{0}C.

3.2 Structural Characterization

Room temperature X-ray diffraction patterns of all the prepared samples are obtained using a Seifert diffractometer and Cu K_α radiation (wavelength λ = 1.5418 Å). Intensity of the diffracted beam is recorded as a function of the 2θ at a step of 0.05^o and a scan rate of 3^o per minute.

The X-ray diffraction pattern of the prepared green colored powder sample at room temperature is shown in Figure 3.3. From this pattern it is found that the prepared green colored powder sample is single phase $Cu(OH)_2$.

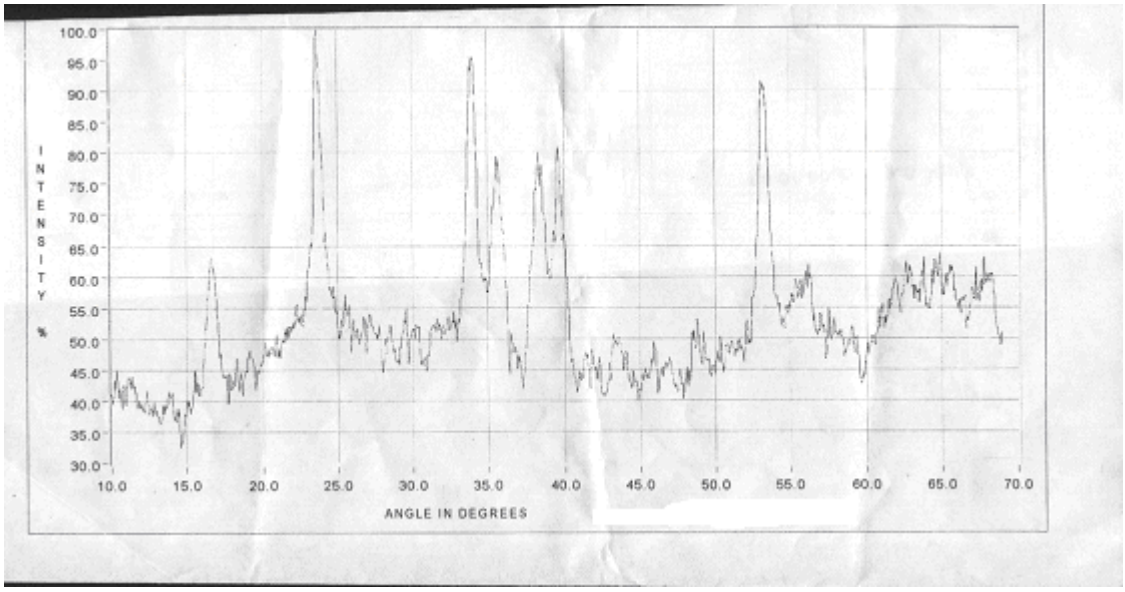

Fig. 3.3: Room temperature X-ray diffraction pattern of $Cu(OH)_2$.

In Section 3.1 it was found that the prepared sample decomposes into some other phase at about 200 ^{0}C. Due to this the $Cu(OH)_2$ sample is heated at 300 and 1000 ^{0}C in air. The X-ray diffraction patterns of the resulting materials are recorded. These are shown in Figures 3.4 and 3.5 respectively. Figure 3.6 shows room temperature X-ray diffraction pattern of bulk CuO powder sample from Aldrich. If the patterns shown in Figures 3.3 and 3.4 are compared with that shown in Figure 3.6 then it is found that the $Cu(OH)_2$ decomposes into CuO on heating above 200 ^{0}C. If Figures 3.4 and 3.6 are compared then it is found that the peaks in Figure 3.4 are broadened compared to those in Figure 3.6. This indicates that the CuO sample prepared by heating $Cu(OH)_2$ at 300 ^{0}C is nanocrystalline. The average crystallite size is calculated by X-ray diffraction line broadening using the modified Scherrer formula [13]

$$d = \frac{0.9\lambda}{\cos\theta_B \sqrt{B_M^2 - B_S^2}}$$

where λ is the wavelength of the X-ray (1.542Å), θ_B is the Bragg angle, B_M is the full width at half-maximum (FWHM) of a peak in radians and B_S is the FWHM of the same peak of a standard sample. Here the CuO powder sample from Aldrich is used as a standard. Two most intense peaks in Figure 3.4 are used to calculate the average crystalline size using the modified Scherrer formula. This turns out to be about 20 nm. The use of $\sqrt{B_M^2 - B_S^2}$ instead of B_M in the Scherrer formula takes care of instrumental broadening.

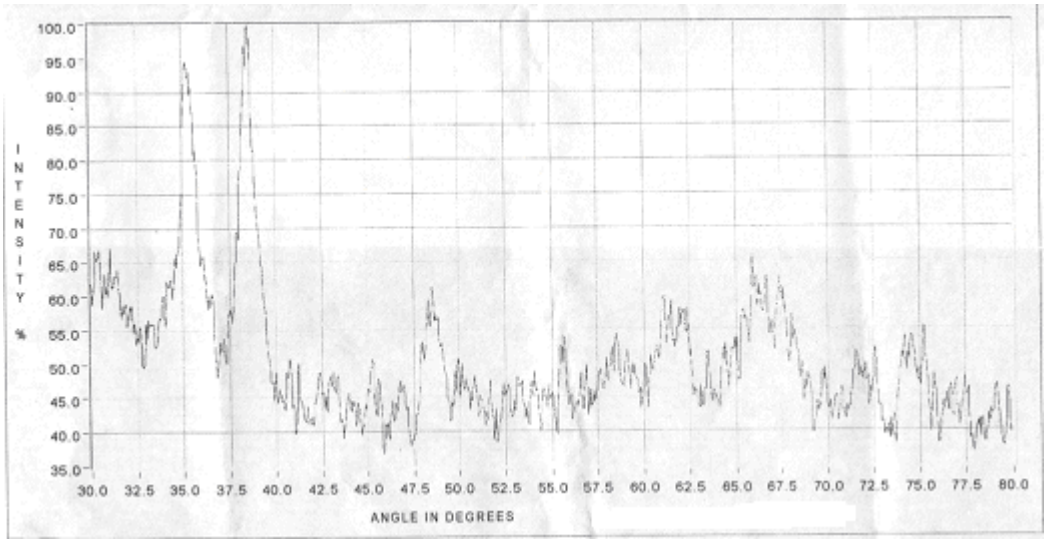

Fig. 3.4: Room temperature X-ray diffraction pattern of material obtained after heating $Cu(OH)_2$ at 300 ^{0}C in air.

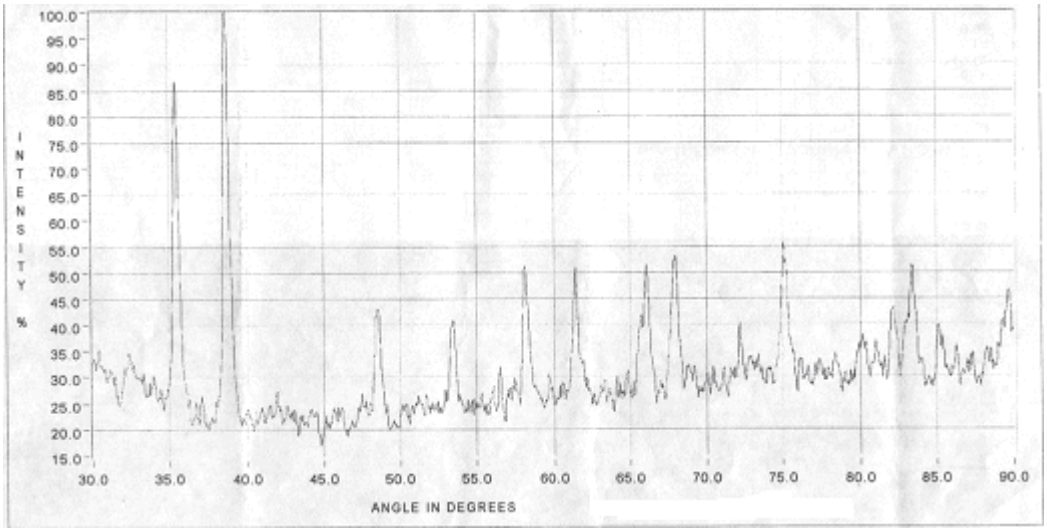

Fig. 3.5: Room temperature X-ray diffraction pattern of material obtained after heating $Cu(OH)_2$ at 1000 ^{0}C in air.

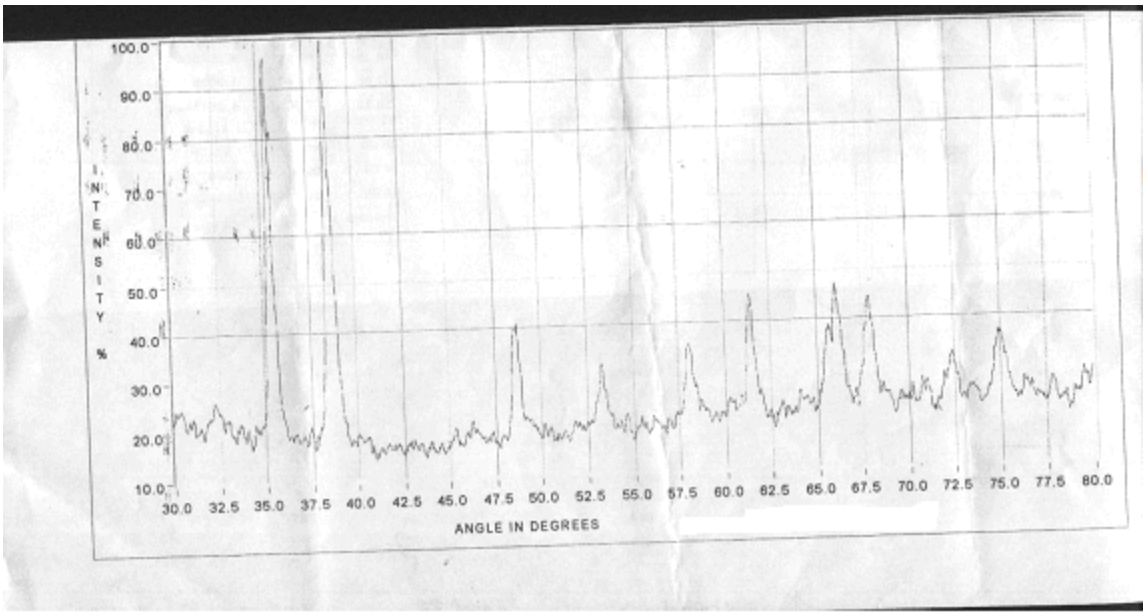

Fig. 3.6: Room temperature X-ray diffraction pattern of bulk CuO.

If Figures 3.5 and 3.6 are compared then it is found that there is hardly any broadening in diffraction peaks in Figure 3.5 compared to that is shown in Figure 3.6. It means that bulk CuO is obtained instead of nanocrystalline CuO due to heating of the $Cu(OH)_2$ at 1000 ^{0}C.

3.3 Magnetization Measurements

Magnetization as a function of magnetic field measurements are done for $Cu(OH)_2$, nanocrystalline CuO and bulk CuO powder samples using a vibrating sample magnetometer at room temperature. These are shown in Figures 3.7, 3.8 and 3.9 respectively. These figures show that there is no hysteresis in all the *M* vs. *H* curves. The magnetizations of the three samples increase with increasing magnetic field strength. It is also observed that at smaller magnetic fields the magnetizations increase with magnetic field nonlinearly whereas at relatively higher magnetic fields the magnetizations increase with magnetic field almost linearly. These are characteristics of antiferromagnetic materials. There is no sign of saturation of magnetizations for these samples because antiferromagnetic materials usually require very high magnetic field to saturate.

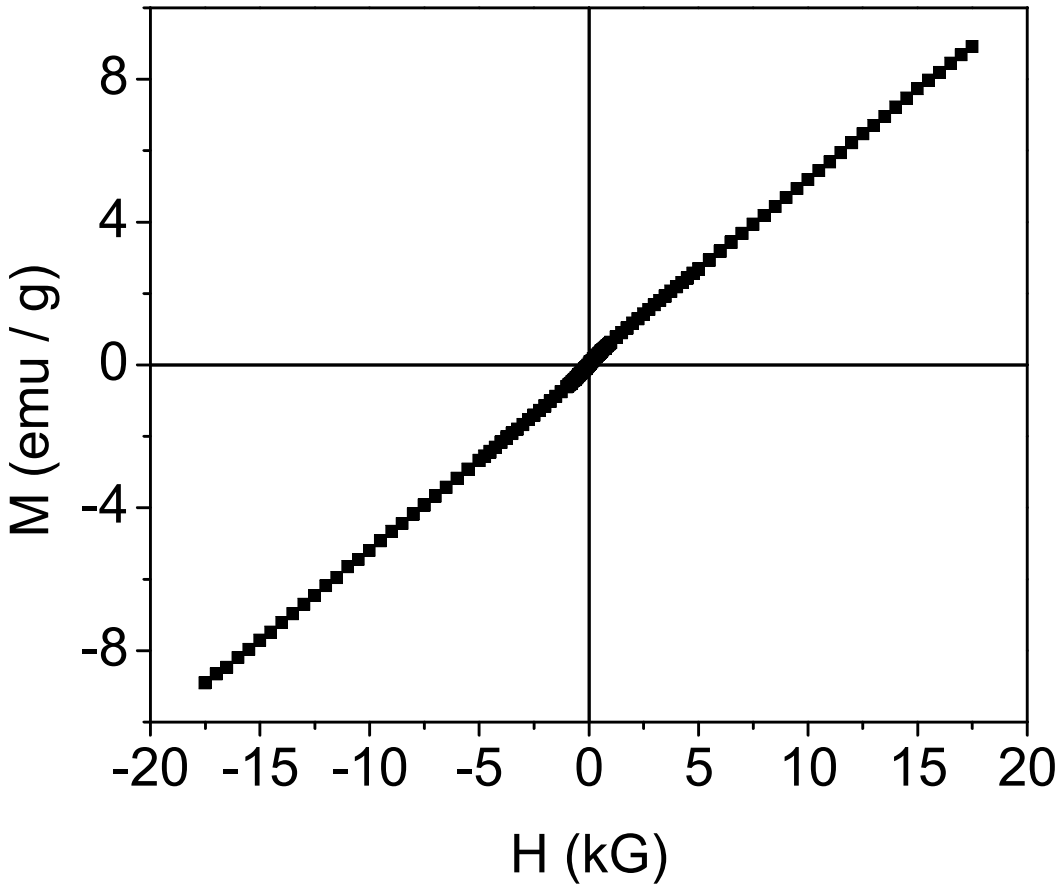

Fig. 3.7: Magnetization versus magnetic field curve for $Cu(OH)_2$ at room temperature.

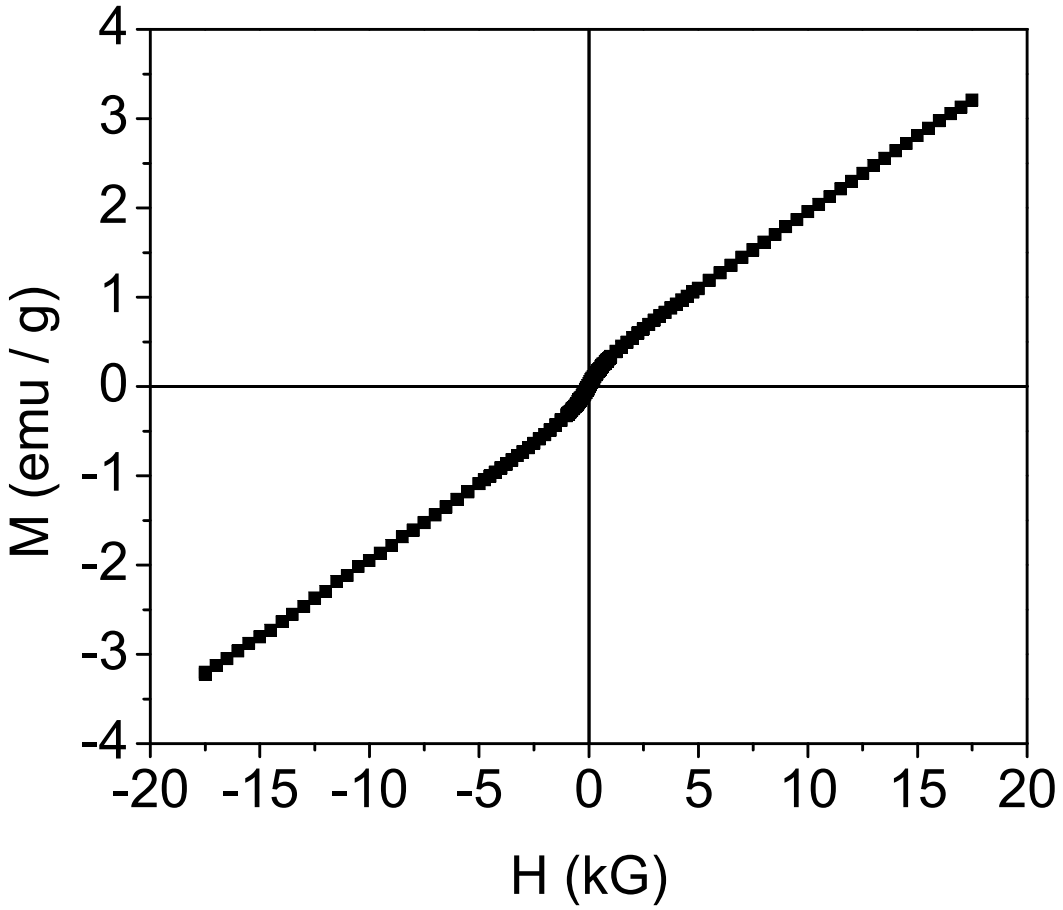

Fig. 3.8: Magnetization versus magnetic field curve for 20 nm CuO particles.

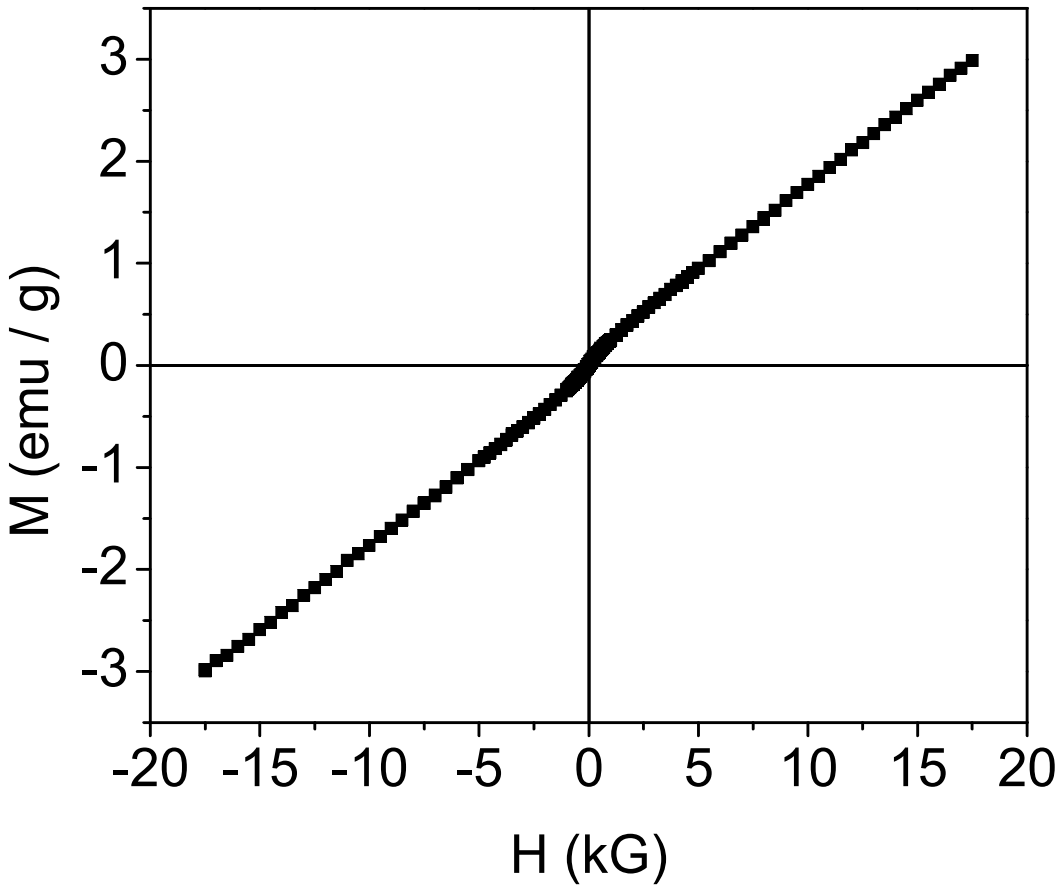

Fig. 3.9: Magnetization versus magnetic field curve for bulk CuO.

Magnetic susceptibility is defined as ratio of the magnetization to the applied magnetic field. For this the linear portion of the magnetization versus magnetic field curve is used. The magnetic susceptibilities of the samples are calculated at room temperature using Figures 3.7, 3.8 and 3.9 and the results are shown in Table I.

Table I: Magnetic susceptibilities of different samples at room temperature.

Sample	Susceptibility (emu / g Oe)
$Cu(OH)_2$	5.0×10^{-4}
Nanocrystalline CuO	1.68×10^{-4}
Bulk CuO	1.63×10^{-4}

If Figures 3.8 and 3.9 are compared then it is found that the magnetization of nanocrystalline CuO is slightly higher than that of bulk CuO. The fraction of spins lying on the surface of antiferromagnetic particles increases with decreasing particle size. Because of this reason the magnetization of antiferromagnetic particles increases with decreasing particle size [14].

CHAPTER-4
CONCLUSIONS

In this work $Cu(OH)_2$, nanocrystalline CuO and bulk CuO powder samples are prepared. The samples are characterized by X-ray diffraction, thermal analysis and vibrating sample magnetometer. The $Cu(OH)_2$ is found to decompose into CuO on heating. This decomposition results into nanocrystalline CuO at lower temperatures and bulk copper oxide at higher temperatures. In this study the $Cu(OH)_2$, nanocrystalline CuO and bulk CuO are found to be antiferromagnetic at room temperature. The magnetization of CuO is also found to increase with decreasing crystallite size.

In literature comparatively little work on $Cu(OH)_2$ is found. In this study the $Cu(OH)_2$ is found to be antiferromagnetic at room temperature. There is still possibility for detailed magnetic study of $Cu(OH)_2$ system by someone in future.

REFERENCES

[1] Magnetic Properties of Fine Particles, edited by J. L. Dormann and D. Fiorani (Elsevier Science, Amsterdam, 1992); Nanophase Materials: Synthesis, Properties, Applications, edited by G. C. Hadjipanayis and R. W. Siegel (Kluwer, Dordrecht, 1994).

[2] L. Neel, in Low Temperature Physics, edited by C. Dewitt, B. Dreyfus, and P. G. de Gennes (Gordon and Breach, New York, 1962).

[3] C. Kittel, Introduction to Solid State Physics (John Wiley and Sons, Inc., 7th ed., 1996).

[4] S. O. Pillai, Solid State Physics (New Age International Publishers, 6th ed., 2005).

[5] I. S. Jacobs and C. P. Beans, in Magnetism, Vol III edited by G. T. Rado and H. Suhl (Academic press inc., New York, 1963).

[6] http://en.wikipedia.org/wiki/Superparamagnetism.

[7] S. Asbrink and L. J. Norrby, Acta Crystallogr., Sect. B: Struct. Crystallogr. Cryst. Chem. **26**, 8 (1970).

[8] http://en.wikipedia.org/wiki/CuO#Crystal_structure.

[9] Nanomaterials: Synthesis, Properties and Applications, edited by A. S. Edelstein and R. C. Cammarata (Institute of Physics Publishing, Bristol and Philadelphia, 1996).

[10] H. Gleiter, Progress in Materials Science, **33**, 223 (1989).

[11] www.msm.cam.ac.uk/phase-trans/2002/Thermal1.pdf.

[12] http://en.wikipedia.org/wiki/Vibrating_sample_magnetometer.

[13] B. D. Cullity, Elements of X-ray Diffraction (Addison-Wesley Publishing Company, Inc., 1956).

[14] S. A. Makhlouf, F. T. Parker, F. E. Spada and A. E. Berkowitz, J. Appl. Phys. **81**, 5561 (1997).